Observing the SO2 and Sulphate Aerosol Plumes from the 2022 Hunga Tonga-Hunga Ha'apai Eruption with IASI

Pasquale Sellitto[1,2], Richard Siddans[3,4], Redha Belhadji[1], Elisa Carboni[3,4], Bernard Legras[5], Aurélien Podglajen[5], Clair Duchamp[5], and Brian Kerridge[3,4]

[1] Univ Paris Est Creteil and Université de Paris, CNRS, LISA, F-94010 Créteil, France

[2] Istituto Nazionale di Geofisica e Vulcanologia, Osservatorio Etneo, Catania, Italy

[3] National Centre for Earth Observation, STFC Rutherford Appleton Laboratory, Chilton, UK.

[4] Remote Sensing Group, STFC Rutherford Appleton Laboratory, Chilton, UK.

[5] Laboratoire de Météorologie Dynamique (LMD-IPSL), CNRS, Sorbonne Université, ENS-PSL, École Polytechnique, Paris, France

Corresponding author: Pasquale Sellitto (pasquale.sellitto@lisa.ipsl.fr)

Key Points:

- Novel co-retrieval of SO_2 and sulphate aerosol from IASI used to study the dispersion of the Hunga Tonga plume over the entire year 2022
- Rapid conversion of SO_2 (two weeks e-folding time) and long-lasting sulphate aerosol plume (no noticeable removal after 1 year) observed
- Larger SO_2 injected mass burden (>1.0 Tg) than previously thought and a large sulphate aerosol total burden (1.6 Tg) estimated

Abstract

The Hunga Tonga-Hunga Ha'apai volcano violently erupted on 15 January 2022, producing the largest perturbation of the stratospheric aerosol layer since Pinatubo 1991, despite the estimated modest injection of SO2. Here we present novel SO_2 and sulphate aerosol (SA) co-retrievals from the Infrared Atmospheric Sounding Instrument, and use them to study the dispersion of the Hunga Tonga plume over the entire year 2022. We observe rapid conversion of SO2 (e-folding time: 17.1±0.6 days) to sulphate aerosols (SA), with an initial injected burden of >1.0 Tg. This points at larger SO2 injections than previously thought. A long-lasting SA plume was observed, with a meridional dispersion of marked anomalies from the tropics to the higher southern hemispheric latitudes. A very small SA removal is observed after 1-year dispersion. The total SA mass burden was estimated at 1.6 ± 0.1 Tg in total column, with a build-up e-folding time of about 2 months.

Plain Language Summary

The eruption of the submarine Hunga Tonga-Hunga Ha'apai (HTHH) volcano in January 2022 polluted the global stratosphere with a large amount of water vapour and volcanic aerosols. In this paper, we present a 1-year long aftermath study of the stratospheric sulphur pollution from this volcanic eruption using observations from the IASI satellite-borne instrument. Gaseous and aerosol sulphur emissions are observed simultaneously using the peculiar potential of this sensor. These observations provide unique capabilities to characterise the aerosol type in the HTHH plume and the sulphur cycle associated with the volcanic emissions. An extremely rapid conversion of gaseous sulphur emissions to aerosols is observed, leading to very large and persistent anomalies of the stratospheric aerosol layer (compared with a consistent long-term climatology), still noticeable in the Southern Hemisphere after 1 year. The total mass of the emitted sulphur in gas and aerosol state is also simultaneously estimated, for the first time.

1 Introduction

After about a month of volcanic unrest, the Hunga Tonga-Hunga Ha'apai (HTHH) volcano (Kingdom of Tonga) violently erupted on 15 January 2022, with a Volcanic Explosivity Index (VEI) of ~6 (Poli and Shapiro, 2022). The specific shallow submarine volcanic setting of HTHH produced a phreato-Plinian eruption, with a very high initial injection reaching up to 55 km (Carr et al., 2022) and an unprecedented amount of ~140 Tg (10% of the overall stratospheric content) of stratospheric water vapour (Khaykin et al., 2022, Millàn et al., 2022). Due to the extremely large water vapour content, extremely fast conversion of volcanic sulphur dioxide (SO_2) emission to sulphate aerosols (SA) was observed (Sellitto et al., 2022) and explained with modelling studies (Zhu et al., 2022). After a few days, the stratospheric aerosol perturbations by the HTHH eruption could be attributed solely to SA, without any optical signature of ash (Sellitto et al., 2022). Small liquid spherical droplets, consistent with SA, where also observed with balloon-borne in situ optical counter measurements during a rapid response campaign at La Réunion island, in the south-western Indian Ocean (Kloss et al., 2022). The HTHH water vapour and SA plumes circumnavigates the Earth in two following weeks and dispersed over the Southern Hemisphere (Khaykin et al., 2022, Legras et al., 2022, Sellitto et al., 2022). Besides the exceptional perturbation in water vapour, the HTHH eruption proved to be the largest perturbation in the stratospheric aerosol layer since Mount Pinatubo eruption in 1991, in particular in the tropics and Southern Hemisphere (Sellitto et al., 2022). This was somewhat surprising because of the limited SO_2 emissions associated with this event, based on first

estimations with early satellite observations (e.g. 0.4 Tg, Carn et al., 2022). Despite the large SA perturbations of the stratospheric aerosol layer, the HTHH plume was associated with an uncommon climate warming effect, due to the large amount of the water vapour perturbations and its infrared radiative emission effect (Sellitto et al., 2022). The HTHH plume radiative effect is also associated with a stratospheric cooling (Schoeberl et al., 2023), a radiatively-driven descent (Sellitto et al., 2022) and a likely detrimental effect on the target of keeping the anthropogenic global warming at 1.5°C in 2030 (Jenkins et al., 2022).

In this paper, we use novel simultaneous SO_2 and SA observations from the high-spectral-resolution infrared space-borne instrument IASI (Infrared Atmospheric Sounding Instrument) to study the SO_2 and SA plume dispersion more than 1 year after the HTHH eruption and to re-estimate their injected burden.

2 Data and Methods

2.1 SO_2 and SA observations with IASI using the RAL IMS scheme

The RAL (Rutherford Appleton Laboratory) Infrared/Microwave Sounder (IMS) retrieval core scheme (Siddans, 2019) uses an optimal estimation spectral fitting procedure to retrieve atmospheric and surface parameters jointly from co-located measurements by IASI (Infrared Atmospheric Sounding Interferometer), AMSU (Advanced Microwave Sounding Unit) and MHS (Microwave Humidity Sounder) on MetOp-B spacecraft, using RTTOV-12 (Radiative Transfer for TOVS) (Saunders et al., 2017) as the forward radiative transfer model. The use of RTTOV-12 enables the quantitative retrieval of volcanic-specific aerosols (SA) and trace gases (SO2). The present paper uses IMS SO2 and SA observations from its near-real-time implementation. The IMS scheme retrieves the SO2 concentration in the sensitive region around 1100–1200 cm^{-1} (in ppbv), assuming a uniform vertical mixing ratio profile. It retrieves sulfate-specific optical depth at 1170 cm^{-1} (i.e. the peak of the mid-infrared extinction cross section; Sellitto and Legras, 2016), assuming a Gaussian extinction coefficient profile shape peaking at 20 km altitude, with 2 km full-width half-maximum. The bulk of the spectroscopic information on SO2 and SA, in the IMS scheme, thus comes from the Infrared Atmospheric Sounding Interferometer (IASI) (Clerbaux et al., 2009). The co-retrieval of SO2 and SA spectroscopic information is crucial to avoid the very large uncertainties on both due to their co-existence in volcanic plume and overlapping spectral signature (Sellitto et al., 2019). As a matter of fact, the weaker SA band at ~900 cm^{-1} must be used in case of exclusive SA retrievals, thus with larger uncertainties due to smaller signal-to-noise ratio with respect to the more intense 1170 cm^{-1} band (Guermazi et al., 2021). At present, only the RAL IMS scheme co-retrieves the two species. The novel IMS SA observations have been found consistent with CALIOP (Cloud-Aerosol Lidar with Orthogonal Polarization) space LiDAR and OMPS (Ozone Mapping and Profiler Suite Limb Profiler) limb instrument (Legras et al., 2022). We refer to the SA optical depth as SA OD in this work. The data are provided daily on a regular grid with 0.25° resolution in latitude and longitude, collecting both the daytime and nighttime swaths. In this paper, averages and percentiles over the period 2007-2018 are provided as climatological reference, and are compared with observation for the full year 2022. Note that the climatological reference is obtained with MetOp-A IASI data. Anomalies associated with the 2022 HTHH eruption are defined as the observations in 2022 minus the 2007-2018 climatology.

2.2 SO_2 and SA total mass burden estimation

The total mass burden of SO_2 and SA (M_{SO2} and M_{SA}) from HT eruption are obtained with IMS observations, considering the latitude interval between the 10°N and 70°S and subtracting a baseline burden before the eruption signature. For short-term analyses of SO_2 rapid conversion, this baseline was taken as the conditions before the eruption (on 13th January), while for the 1-year SA analysis, the SA OD anomaly is considered (thus climatological baseline is subtracted out).

While the calculation of the SO_2 mass burden is straightforward, assumptions on some chemical and physical properties of the SA particles are needed to estimate the SA mass burden. The SA mass burden is calculated using the following equation:

$$M_{SA} = \text{SA OD}/\langle \text{MEE} \rangle \quad \text{(Eq. 1)}$$

An average mid-infrared mass aerosol extinction efficiency ($\langle MEE \rangle$) centred around the peak SA absorption band at 1170 cm^{-1} is obtained with the Oxford Mie routines (available at the following website: http://eodg.atm.ox.ac.uk/MIE/) and using Eq. 2 (see its derivation in Clyne et al., 2021).

$$\langle \text{MEE} \rangle = \frac{3}{4 * \rho_p * r_{\text{eff}}} * Q_{ext}(r_{\text{eff}}) \quad \text{(Eq. 2)}$$

In Eq. 2, ρ_p is the SA average mass density taken as 1.75 g cm^{-3} (a typical value for a sulphuric acid percent weight 70% and lower-stratospheric temperatures, see Duchamp et al., 2023), r_{eff} is the effective radius of the SA particles and Q_{ext} is the extinction efficiency factor calculated with the Mie code. Using a typical r_{eff} for the HTHH plume of 0.45 µm (see Duchamp et al., 2023), we obtain a $\langle MEE \rangle$ of 0.27 $m^2 g^{-1}$. While, in general, the MEE depends critically on the particles mean size in terms of r_{eff}, we have found that for typical mid-infrared values and HTHH r_{eff}, its variability is very limited (<3% $\langle MEE \rangle$ variability for r_{eff} between 0.3 and 0.6 µm). This limits the SA total mass burden systematic uncertainties associated with the SA size distribution assumption. Limited systematic uncertainties can be associated with the assumption of ρ_p.

3 Results

3.1 SO_2 and SA anomalies induced by the HTHH eruption at the hemispheric scale

Legras et al. (2022) and Sellitto et al. (2022) (see e.g. Fig. 3a of this latter paper) observed the rapid conversion of the SO_2 emission from HTHH eruption to SA. Detections of SO_2 exceeding a relatively small threshold (2 DU) are not visible from IASI observations after the end of January, i.e. about two weeks after the eruption (Fig. S1). Since February 2022, SA dominate the sulphur plume and must be used to study its dispersion at the hemispheric scale at longer timescales than a few weeks. Figure 1a shows the monthly mean SA OD anomaly for the year 2022. A distinct anomaly in SA OD due to the HTHH eruption, reaching values larger than 0.005 in February/March can be seen. The SA OD anomaly is initially located in the latitude band between 0 and 25°S, where the HTHH volcano is located, and then progressively spreads towards southern hemispheric mid-latitudes and high-latitudes, after June 2022. The SA OD anomalies appear longitudinally well mixed since February, thus supporting the evidence of a rapid initial circumnavigation of the Earth, as reported by Legras et al. (2022) and Khaykin et al. (2022). The zonal transport of the HTHH plume is quicker than what observed for recent moderate eruptions, like Nabro 2011 (circumnavigation in ~2 month, Bourassa et al., 2012) and

Raikoke 2019 (~1 month, Kloss et al., 2021). The meridional dispersion dynamics of the HTHH plume can be seen in a compact manner with SA OD anomalies zonal means in Fig. 1b. In contrast with the zonal transport, meridional dispersion at the southern hemispheric scale is significantly slower that for recent moderate stratospheric eruptions, reaching high-latitudes after 6 months. The HTHH plume crossed only marginally the equator and the northern hemispheric stratospheric aerosol layer is not significantly perturbed by this event (see also Fig. 3e in Sellitto et al., 2022). Two distinct phases in the build-up of the SA plume seem to appear, one in February/March at 10-20°S and one in July/August at 30-50°S. This second late build-up phase is still to be fully understood and studies are ongoing.

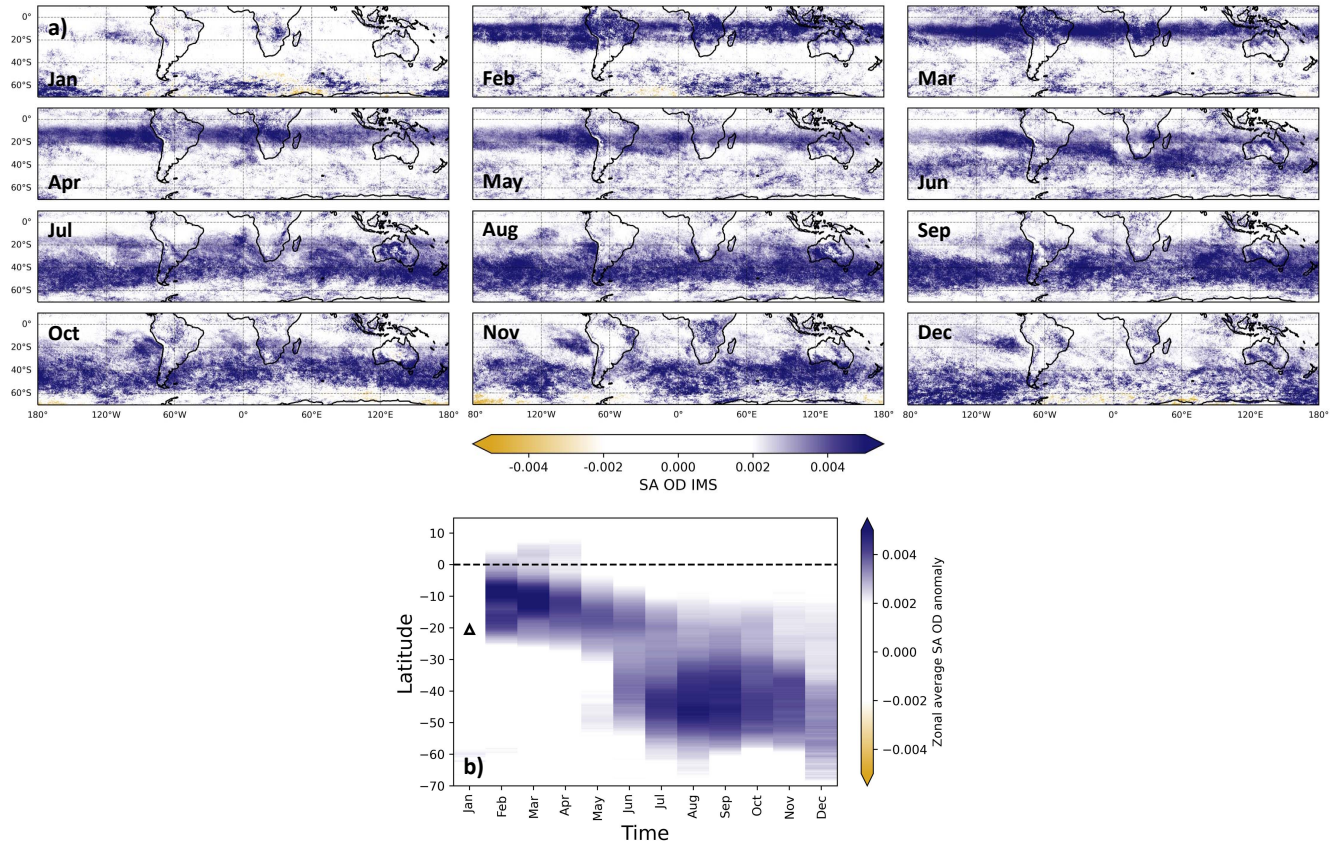

Figure 1: (a) Monthly mean SA OD anomaly from IASI observations in 2022, from 10°N to 70°S. (b) Zonal average SA OD anomaly from IASI observations in 2022, in the same latitude range as panel a. The month/latitude position of the HTHH eruption in indicated as a black triangle.

The spatiotemporal propagation of the SA OD perturbations discussed above can also be seen by directly comparing zonal average values of the SA OD in 2022 and for the 2007-2018 climatology (Fig. S2). While a perturbation is not clearly visible in January, a pronounced perturbation, largely exceeding the 5-95 percentile interval of climatology, appears in February between the equator and 30°S and then spreads gradually to higher latitudes in the Southern Hemisphere. Figure 2 shows average values in selected latitude regional bands. The Northern Hemisphere does not look affected by the HTHH eruption throughout the year 2022 (a perturbation during the first months of 2022 can be seen at northern hemispheric mid-latitudes but seems unrelated with the HTHH eruption). Very large perturbations can be seen since January in the tropics and since April in southern hemispheric mid-latitudes. A limited

perturbation is also visible since April for southern hemispheric high-latitudes. The whole Southern Hemisphere is still perturbed by December 2022, except for very high latitudes.

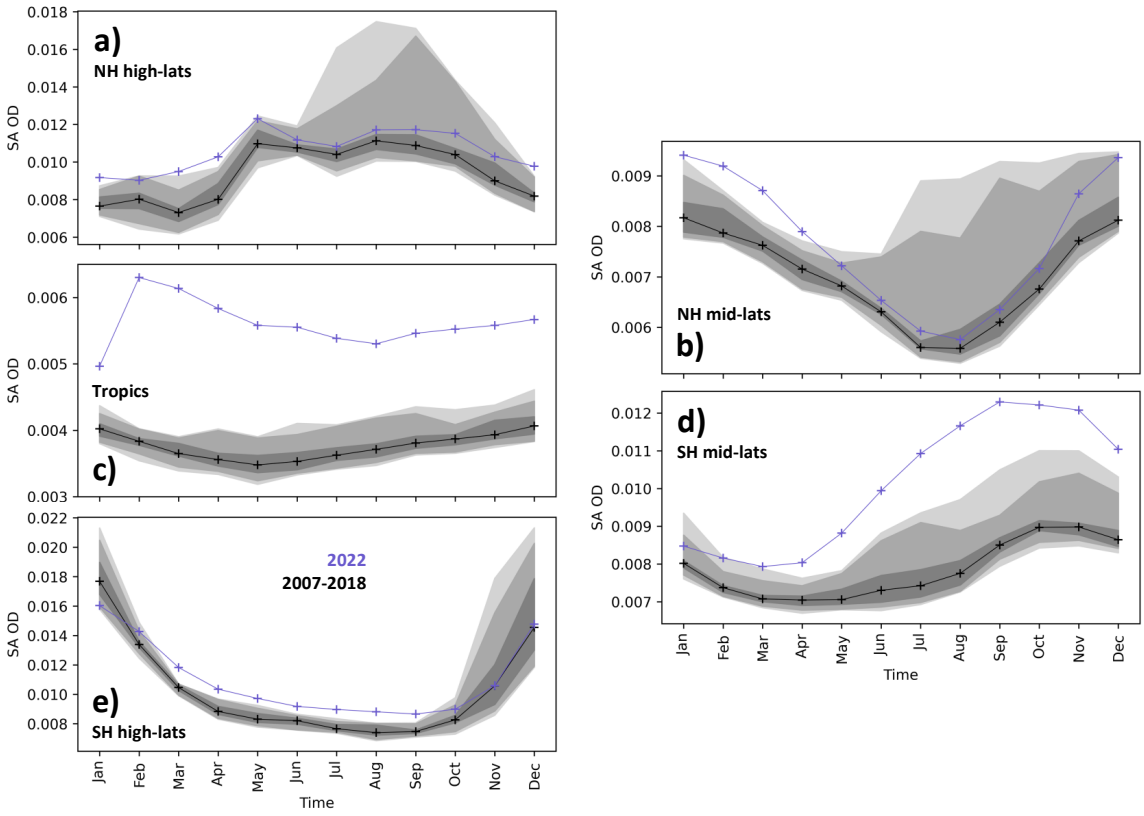

Figure 2: Regional monthly mean IASI SA OD in 2022 (blue lines and crosses), and median values (black lines and crosses), 5-95 (dark grey shaded area), 10-90 (medium grey shaded area) and 30-70 (light grey shaded area) percentiles intervals for the period 2007-2018, in the five latitude regions: Northern Hemispheric high-latitudes (panel a), Northern Hemispheric mid-latitudes (panel b), tropics (panel c), Southern Hemispheric mid-latitudes (panel d) and Southern Hemispheric high-latitudes (panel d).

3.2 The sulphur cycle in the HTHH plume

Figures 3a-b show the short-term (from the eruption to late February) evolution of the estimates SO2 and SA total mass burdens. For such an almost instantaneous explosive events, the SO2 mass burden is expected to reach its maximum in the very first days and then exponentially decrease due to chemical sink associated with the conversion to SA, as described in Eq. 1.

$$M_{SO2}(t) = M_{SO2}(t_0) * e^{\frac{-t}{\tau SO2}} \quad \text{(Eq. 1)}$$

In Eq. 1, $M_{SO2}(t)$ and $M_{SO2}(t_0)$ are the mass burden at a given time and the total mass burden injected at the time of the eruption, and τ_{SO2} is the e-folding time due to chemical conversion to SA. A surprising feature of the IASI-estimated HTHH SO2 mass burden evolution is that a clear maximum is not observed immediately after the eruption but a few days later, i.e. on 19 January. The total mass burden on 15 January is about 0.45 Tg, very close to the initial SO2 mass burden estimation of Carn et al. (2022) with Sentinel-5p TROPOMI (TROPOspheric Monitor Instrument), which is the present reference of the injected SO2 from the HTHH eruption. The

larger values in the days after the eruption, reaching values as large as 1.0 Tg, might point at an initial underestimation of the SO2 total injected mass burden, possibly due to ash- or water-vapour-induced opacity of the very young plume. Our results suggest that the injected SO2 mass burden of the HTHH eruption are likely larger than thought and a 1.0 Tg lower limit is more realistic. A parameterised exponential decay function, as the one of Eq. 1, was fitted to the SO2 mass burden data (starting from 18 January, see Fig. 3a) to obtain an injected SO2 mass of 1.0 ± 0.1 Tg and an e-folding time of 17.1 ± 0.6 days (see Tab. 1). This latter value suggests a 2-to-3 times faster chemical sink due to conversion to SA than expected at the HTHH plume's altitudes (e.g. Carn et al., 2016). The fast conversion to SA is a known feature of the HTHH plume, attributed to the large amount of water vapour due to the phreatic nature of this event (e.g. Sellitto et al., 2022, Zhu et al., 2022).

Figure 3b shows the temporal evolution of the SA mass during the whole year 2022. The SA plume build-up is modelled by the exponential function of Eq. 2, where $M_{SA}(t)$ and $M_{SA}(t_\infty)$ are the SA mass burden at a given time and the total SA mass burden after full build-up of the plume, and τ_{SA} is the build-up e-folding time. It is assumed that SA sinks (gravitational settling, evaporation and others) are not effective at the 1-year time scale.

$$M_{SA}(t) = M_{SA}(t_\infty) * \left(1 - e^{\frac{-t}{\tau_{SA}}}\right) \quad \text{(Eq. 2)}$$

Fitting Eq. 2 to the SA mass burden data, we obtain an injected SA mass of 1.6 ± 0.1 Tg and a build-up e-folding time of 60.1 ± 21.1 days (see Tab. 1), i.e. ~2 months. Sellitto et al. (2022) proposed a range of values between 1.0 and 3.0 Tg for the SA mass burden, depending on the particles size. There is now increasing consensus that HTHH average particles size does not exceed 0.5 μm (e.g. Taha et al., 2022, Duchamp et al., 2023), which reduces uncertainties on the MEE (see Sect. 2.2) and places the SA mass burden in the middle of that previous range. Using limb-satellite SAGE III/ISS observations, Duchamp et al. (2022) estimated the stratospheric H_2SO_4 total mass at a maximum of ~0.7 Tg which corresponds, with the assumption of a H_2SO_4 weight percentage of 70%, to a stratospheric SA mass of ~1.0 Tg. Our present estimate is obtained with a nadir-viewing instrument and is representative of the total tropospheric-plus-stratospheric column. To compare the two estimates, we made a crude estimation of the proportion of HTHH aerosols in the troposphere and stratosphere using OMPS data (Fig. S3). Taking e.g. zonal average AOD observations in March (Fig. S3d), we estimate that ~45% of the total column aerosols are in the stratosphere. With this assumption, our IASI SA mass burden distributes as ~0.9 Tg in the troposphere and ~0.7 Tg in the stratosphere. This latter value is consistent with SAGE III/ISS estimations of Duchamp et al. (2023), even if slightly smaller. It is worth noting that the OMPS-based repartition of SA in troposphere and stratosphere is very crude, in particular due the possibility of cloud contamination in the troposphere, so this has to be taken with caution. In general, a 1.0 Tg mass burden of SO2, if totally converted to SA with 70% H_2SO_4 weight percentage would lead to ~2.2 Tg of SA. Thus, our 1.6 Tg SA mass burden estimate points at a ~30% lower values than in case of full SO2 conversion to SA, possible due to either issues with IASI SA OD sensitivity or to an additional sink for SO2 or SA.

It is interesting to notice that the two distinct build-up phases of the SA plume discussed in Sect. 3.1 in terms of the SA OD are also visible in the SA mass burden evolution (Fig. 3c, see maxima in February and in August). This latter evidence excludes the possibility that this effect is due merely to meridional transport.

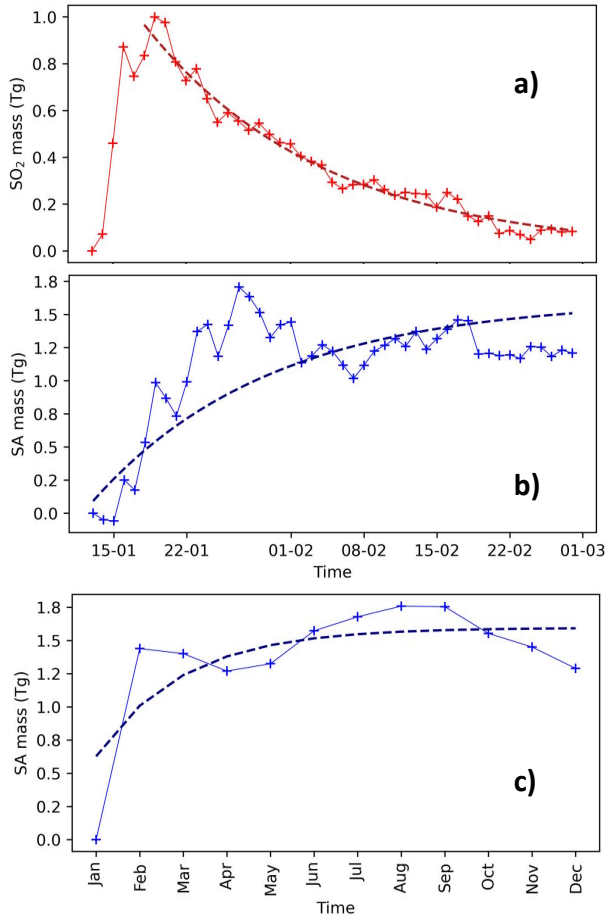

Figure 3: (a,b) Short term (January and February 2022) temporal evolution of SO2 (panel a) and SA (panel b) total masses, estimated using daily IASI observations. (c) Long term (year 2022) temporal evolution of SA total mass, estimated with montly average IASI observations. In panels a-c, fit of parameterisation functions of the total masses evolution is also shown, see text for more details.

Table 1: Estimated SO_2 and SA total injected masses (M_{SO2} and M_{SA}, respectively), SO_2 decay e-folding time (τ_{SO2}) and SA build-up e-folding time (τ_{SA}), based on the parameterisation shown in Fig. 3.

M_{SO2}	1.0 ± 0.1 Tg
τ_{SO2}	17.1 ± 0.6 days
M_{SA}	1.6 ± 0.1 Tg
τ_{SA}	60.1 ± 21.1 days

Using these novel AOD estimation in the thermal infrared in combination with total column AOD observations in the visible spectral range of e.g. OMPS-LP (Fig. S3), a shortwave-to-longwave average Ångström Exponent (AE) cans be estimated. For the month of March 2022, when the build-up of the plume is almost completed, we obtain visible and infrared AODs of

0.044 and 0.0026, with an AE of 1.13 (Tab. S1). Similar values of the AE were obtained in the visible range alone by Taha et al. (2022).

5 Conclusions

In this paper, we have presented novel IASI SO_2/SA co-retrievals, that were used to track and analyse the sulphur plume emanated from the record-breaking HTHH eruption of 15 January 2022. The full year 2022 of retrievals is used here. We observed a rapid conversion of SO2 to SA, with an estimated e-folding time of 17.1±0.6 days – a clear SO2 signal is not observable since February 2022. We estimated a lower limit 1.0 Tg for the initial injected SO2 burden, which is larger than previous estimates with ultraviolet/visible nadir instruments. This can be due to an initially large opacity of the plume, due to large ash and water vapour content in the early plume. Starting from February 2022, we observed a long-lasting SA plume. The plume circumnavigated the Earth rapidly (1-month time scale) and dispersed meridionally more slowly. Marked anomalies in SA OD, with respect to a 2007-2018 climatology, are observed in the tropics, for the whole 2022, and at southern hemispheric mid- and high-latitudes starting from April 2022. Overall, a very small SA removal is observed after 1-year of plume dispersion. The total SA mass burden was estimated at 1.6 ± 0.1 Tg in total column, with possibly ~45% in the stratosphere (~0.7 Tg) and the remaining ~55% in the troposphere (~0.9 Tg). The build-up e-folding time of the SA plume was estimated at ~2 months. Using the new infrared SA OD obtained with IASI and the visible AOD with OMPS-LP, we estimated a broad-band AE of ~1.13 in March 2022, which is consistent with previous visible-only AE estimations and relatively (around 0.5 µm on average) large SA particles.

Acknowledgments

This research has been supported by the Agence Nationale de la Recherche (grant no: 21-CE01-0007-01, ASTuS), the Centre National d'Études Spatiales (CNES) via TOSCA/IASI grant, the Centre national de la recherche scientifique-Institut National des Sciences de l'Univers (CNRS-INSU PNTS (Programme National de Télédétection Spatiale) via MIA-SO2 grant. The IMS scheme development was funded by the UK National Centre for Earth Observation (NCEO, grant numbers NE/R016518/1 and NE/N018079/1). IMS retrievals were produced using JASMIN, the UK collaborative data analysis facility, at the Rutherford Appleton Laboratory.

Open Research

The IMS/IASI SO2 and SA OD datasets used in this work (L2 format) can be accessed through the CEDA database (https://catalogue.ceda.ac.uk/uuid/489e9b2a0abd43a491d5afdd0d97c1a4). The OMPS-LP data are freely available from EarthData centre at: https://disc.gsfc.nasa.gov/datasets/OMPS_NPP_LP_L2_AER_DAILY_2/summary.

References

Bourassa A.E., Robock A., Randel W.J., Deshler T., Rieger L.A., Lloyd N.D., Llewellyn E.J., Degenstein D.A. (2012). Large volcanic aerosol load in the stratosphere linked to Asian monsoon transport. Science. 2012 Jul 6;337(6090):78-81. doi: 10.1126/science.1219371

Carn, S. A., Clarisse, L. & Prata, A. J. (2016) Multi-decadal satellite measurements of global volcanic degassing. J. Volcanol. Geotherm. Res. 311, 99–134.

Carn, S., Krotkov, N., Fisher, B. & Li, C. (2022) Out of the blue: volcanic SO2 emissions during the 2021-2022 eruptions of Hunga Tonga - Hunga Ha'apai (Tonga). Front. Earth Sci. 10, https://doi.org/10.3389/feart.2022.976962.

Carr, J. L., Horvath, A., Wu, D. L., & Friberg, M. D. (2022). Stereo Plume Height and Motion Retrievals for the Record-Setting Hunga Tonga-Hunga Ha'apai Eruption of 15 January 2022. Geophysical Research Letters, 49 ,270 e2022GL098131. doi: 10.1029/2022GL098131

Clerbaux, C., Boynard, A., Clarisse, L., George, M., Hadji-Lazaro, J., Herbin, H., Hurtmans, D., Pommier, M., Razavi, A., Turquety, S., Wespes, C., and Coheur, P.-F. (2009) Monitoring of atmospheric composition using the thermal infrared IASI/MetOp sounder, Atmos. Chem. Phys., 9, 6041–6054, https://doi.org/10.5194/acp-9-6041-2009.

Clyne, M., Lamarque, J.-F., Mills, M. J., Khodri, M., Ball, W., Bekki, S., Dhomse, S. S., Lebas, N., Mann, G., Marshall, L., Niemeier, U., Poulain, V., Robock, A., Rozanov, E., Schmidt, A., Stenke, A., Sukhodolov, T., Timmreck, C., Toohey, M., Tummon, F., Zanchettin, D., Zhu, Y., and Toon, O. B. (2021): Model physics and chemistry causing intermodel disagreement within the VolMIP-Tambora Interactive Stratospheric Aerosol ensemble, Atmos. Chem. Phys., 21, 3317–3343, https://doi.org/10.5194/acp-21-3317-2021.

Duchamp, C., Wrana, F., Legras, B., Sellitto, P., Belhadji, R., von Savigny, C. (2023) Observation of the aerosol plume from the 2022 Hunga Tonga - Hunga Ha'apai eruption with SAGE III/ISS. ESS Open Archive, doi: 10.22541/essoar.168771425.59096731/v1

Guermazi, H., Sellitto, P., Cuesta, J., Eremenko, M., Lachatre, M., Mailler, S., Carboni, E., Salerno, G., Caltabiano, T., Menut, L. et al. (2021) Quantitative Retrieval of Volcanic Sulphate Aerosols from IASI Observations. Remote Sensing, 13, 1808. https://doi.org/10.3390/rs13091808

Jenkins, S., Smith, C., Allen, M. et al. (2023). Tonga eruption increases chance of temporary surface temperature anomaly above 1.5 °C. Nat. Clim. Chang. 13, 127–129, https://doi.org/10.1038/s41558-022-01568-2

Khaykin, S., Podglajen, A., Ploeger, F., Grooß, J.-U., Tence, F., Bekki, S., . . ., Ravetta, F. (2022). Global perturbation of stratospheric water and aerosol burden by Hunga eruption. Communications Earth & Environment, 3 (1), 316, doi: 10.1038/s43247-022-00652-x

Kloss, C. et al. (2021) Stratospheric aerosol layer perturbation caused by the 2019 Raikoke and Ulawun eruptions and their radiative forcing. Atmos. Chem. Phys. 21, 535–560.

Kloss, C., Sellitto, P., Renard, J.-B., Baron, A., Bègue, N., Legras, B., . . . Jégou, F. (2022). Aerosol Characterization of the Stratospheric Plume From the Volcanic Eruption at Hunga Tonga 15 January 2022. Geophysical Research Letters, 49 (16), e2022GL099394. doi: 10.1029/2022GL099394

Legras, B., Duchamp, C., Sellitto, P., Podglajen, A., Carboni, E., Siddans, R., . . ., Ploeger, F. (2022). The evolution and dynamics of the Hunga Tonga–Hunga Ha'apai sulfate aerosol plume

in the stratosphere. Atmospheric Chemistry and Physics, 22 (22), 14957–14970. doi: 10.5194/acp-22-14957-2022

Millàn, L., Santee, M. L., Lambert, A., Livesey, N. J., Werner, F., Schwartz, M. J.,. . . Froidevaux, L. (2022). The Hunga Tonga-Hunga Ha'apai Hydration of the Stratosphere. Geophysical Research Letters, 49 (13), e2022GL099381. doi:10.1029/2022GL099381

Poli, P., & Shapiro, N. M. (2022). Rapid Characterization of Large Volcanic Eruptions: Measuring the Impulse of the Hunga Tonga Ha'apai Explosion FromnTeleseismic Waves. Geophysical Research Letters, 49 (8), e2022GL098123. doi:10.1029/2022GL098123

Schoeberl, M. R., Wang, Y., Ueyama, R., Taha, G., Jensen, E., & Yu, W. (2023). Analysis and Impact of the Hunga Tonga-Hunga Ha'apai Stratospheric Water Vapor Plume. Geophysical Research Letters, 49 (20), e2022GL100248. doi:doi.org/10.1029/2022GL100248

Sellitto, P. & Legras, B.(2016) Sensitivity of thermal infrared nadir instruments to the chemical and microphysical properties of UTLS secondary sulfate aerosols, Atmos. Meas. Tech., 9, 115–132, https://doi.org/10.5194/amt-9-115-2016.

Sellitto, P., Guermazi, H., Carboni, E., Siddans, R., and Burton, M. (2019) Unified quantitative observation of coexisting volcanic sulfur dioxide and sulfate aerosols using ground-based Fourier transform infrared spectroscopy, Atmos. Meas. Tech., 12, 5381–5389, https://doi.org/10.5194/amt-12-5381-2019.

Sellitto, P., Podglajen, A., Belhadji, R., Boichu, M., Carboni, E., Cuesta, J., . . ., Legras, B. (2022). The unexpected radiative impact of the Hunga Tonga eruption of 15th January 2022. Communications Earth & Environment, 3 (1), 288, doi: 10.1038/s43247-022-00618-z

Siddans, R. (2019) Water Vapour Climate Change Initiative (WV_cci) - Phase One, Deliverable 2.2; Version 1.0, 27 March 2019, https://climate.esa.int/documents/1337/Water_Vapour_CCI_D2.2_ATBD_Part2-IMS_L2_product_v1.0.pdf

Taha, G., Loughman, R., Colarco, P. R., Zhu, T., Thomason, L. W., & Jaross, G. (2022). Tracking the 2022 Hunga Tonga-Hunga Ha'apai Aerosol Cloud in the Upper and Middle Stratosphere Using Space-Based Observations. Geophysical Research Letters, 49 (19), e2022GL100091. doi: 10.1029/2022GL100091

Zhu, Y., Bardeen, C. G., Tilmes, S., Mills, M. J., Wang, X., Harvey, V. L., . . . Toon, O. B. (2022). Perturbations in stratospheric aerosol evolution due to the water-rich plume of the 2022 Hunga-Tonga eruption. Communications Earth & Environment, 3 (1), 248. doi: 10.1038/s43247-022-00580-w